

DYE SENSITIZED SOLAR CELLS WITH HIGH PHOTO-ENERGY CONVERSION -CONTROLL OF NANO-PARTICLE SURFACES-

Shuzi HAYASE

Kyushu Institute of Technology, 2-4, Hibikino, Wakamatsu-ku, Kitakyuushu 808-0196 Japan

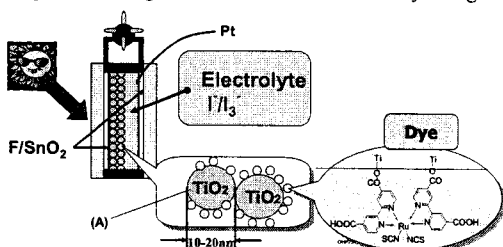
ABSTRACT

Some of factors affecting photo-conversion efficiency of dye sensitized solar cells (DSCs) are discussed in terms of TiO_2 electrodes. The first topic is on the surface modification of TiO_2 nano-particles, which is associated with electron traps on the surface of TiO_2 nano-particles. The surface is modified with dye molecules under pressurized CO_2 atmosphere to increase the surface coverage of TiO_2 nano-particles with dye molecules. This increases J_{sc} because of an increase in the amount of dye molecules and a decrease in the amount of trapping sites on TiO_2 nano-particles. In addition, the decrease in the amount of trap sites increases V_{oc} because decreases in V_{oc} are brought about by the recombination of I_2 molecules with electrons trapped on the TiO_2 surfaces. Selective staining for tandem cells is proposed. The second topic is on the contact between a SnO_2/F transparent conductive layer (TCL) and nano-particles. Polishing the TCL surfaces with silica nano-particles increases the contact, resulting in J_{sc} increases. The third topic is the fabrication of ion-paths in TiO_2 layers. Electro-spray coating of TiO_2 nano-particles onto TCL is shown to be effective for fabricating ion-paths in TiO_2 layers, which increases J_{sc} .

INTRODUCTION

Photo-conversion efficiencies of dye sensitized solar cells (DSCs) reached the value over 10%. DSC is expected to be one of solar cells for next generation because of the economical fabrication processes. One of the crucial development items is to increase the photo-conversion efficiencies. In this presentation, we focused on TiO_2 layers. Our purpose is to show the direction of how to design the TiO_2 layers to improve the photo-conversion efficiency.

Figure 1 shows the DSC structure. The DSC consists of a F-doped SnO_2 (F/SnO_2) transparent conductive layer, a TiO_2 layer covered with mono-layered dye molecules, electrolytes, a Pt layer and a F/SnO_2 layer. The mechanism for photovoltaic generation is summarized briefly in Figure 2.



OHP1301

B. O'Regan and M. Graetzel *Nature*, 1991, 353, 737

Figure 1 DSC structure

Photo-excited electrons are injected from dye molecules to TiO_2 layers. Electrons diffuse in cumulated TiO_2 nano-

particles to reach an anode. On the counter electrode, electrons are transferred to I_2 (I_3^-) which is reduced to I^- . I^- diffuses in an electrolyte layer to give electrons to photo-oxidized dye molecules. A serious performance deterioration is brought about by back electron transfers from TiO_2 layers to $\text{I}_2(\text{I}_3^-)$ species in electrolytes. Therefore, in order to increase the efficiency, following items are

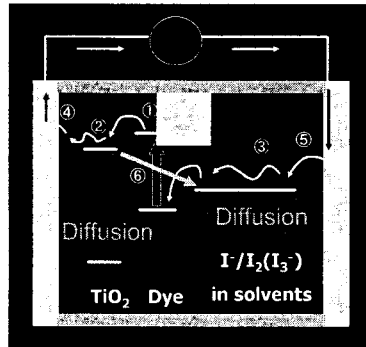


Figure 2 Mechanism of photovoltaic generation

considered.

- ✓ Increase in diffusion coefficients of electrons in TiO_2 layers and $\text{I}_2(\text{I}_3^-)$ species in a electrolyte layer (2 and 3 in Figure 2).
- ✓ Decrease in an interfacial resistance between a F/SnO_2 conductive layer and TiO_2 nano-particles (4 in Figure 2).
- ✓ Decrease in an interfacial resistance between a counter electrode and $\text{I}_2(\text{I}_3^-)$ species in a electrolyte layer (5 in Figure 2).
- ✓ Decrease in back electron transfer reactions (6 in Figure 3).

Among them, we focused on TiO_2 electrodes which affect 1, 2, 4 and 6 in Figure 2.

DYE ADSORPTION UNDER PRESSURIZED CO_2

In order to increase short circuit current (J_{sc}), the amount of electrons injected from dye molecules have to be increased. Many researchers have tried to synthesize dye molecules absorbing wide range of wavelengths of sun light. Actually, this should be the best method to increase the amount of injected electrons. For example, various Ru complex dyes²⁻⁵ and organic dyes⁶⁻¹⁰ have been reported for DSC. Among them, N3 dyes (cis-di(thiocyanato)-N,N'-bis(2,2'-bipyridyl-4,4'-dicarboxylato)ruthenium(II)) and black dye ((C4H9)4N)3(Ru(Htcterpy)(NCS)3) (tcterpy = 4,4',4''-tricarboxy-2,2',2''-terpyridine) are the representative dyes. The latter has visible absorption extending into near-IR region up to 900 nm and 10.4% efficiency has been reported^{11,12}. Another conceivable method to improve efficiencies is to increase the amount of dye molecules

adsorbed on porous TiO₂ layers. The adsorption is commonly carried out by dipping porous TiO₂ substrates in dye solutions. Dipping time reaches several hours to several days, depending on dye structures. We aimed at bonding Ru dyes to the inner part of TiO₂ nano-pores effectively by use of pressurized CO₂ atmosphere. It has been reported that molecular diffusions are fast like gases and molecular concentrations are high like fluids in supercritical CO₂¹³. Bando and her coworkers used supercritical CO₂ to stain organic dyes (eosin Y) on porous TiO₂ layers. They have reported improved photo-voltaic performances. However, the photocurrent was low (3.5 mA/cm²). In this sense, black dye and N3 dye are essential for realizing high performance DSCs. As far as I know, there is no report on staining Ru complexes under a pressurized CO₂ atmosphere. Figure 3 shows our goal for TiO₂ layers. If the coverage of TiO₂ nano-particles with dye molecules increases under a pressurized CO₂ atmosphere, the amount of electrons injected from dye molecules increase, resulting in increasing J_{sc}. In addition, the amount of electron traps on the surface of TiO₂ particles would decrease, resulting in increasing open circuit voltage (V_{oc}).

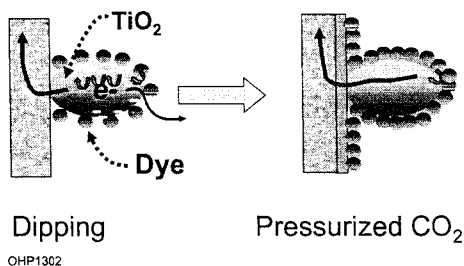


Figure 3 Expected TiO₂ nano-particles covered with dye molecules

Ti-Nanoxide D paste (Solaronix SA) was coated on SnO₂/F layered glasses (30 ohm/square, Nippon Sheet Glass Co. Ltd). The substrates were baked at 450 °C to fabricate 9 micron thickness of TiO₂ layers. The substrate and N3 or black dye (3 x 10⁻⁴ M in t-butylalcohol and acetonitrile (1:1 (vol/vol))) were separately put in a stainless container. CO₂ gas was introduced into the container. The substrate was stained under 24 Mpa at 40 °C. It has been reported that supercritical CO₂ phase appears above 7.38 Mpa and 31.1 °C. The substrate was rinsed fully in the mixture of t-butylalcohol and methanol (1:1(vol/vol)). Adsorption by a dipping method was carried out by immersing substrates in dye solution of t-butyl alcohol/acetonitrile(1:1 (vol/vol)) solution (3 x 10⁻⁴ M) at room temperature. Pt sputtered SnO₂/F layered glass substrates were employed as counter electrodes. An electrolyte was inserted into the cell at room temperature. The electrolyte consisted of I₂ (40mM), LiI(500mM), t-butylpyridine (580mM) in acetonitrile. The cell area was 0.25 cm². After the cell fabrication, the cell area was precisely calculated by using photograph. Photo-electrochemical measurements were performed using a solar simulator (YSS-50A, Yamashita Denso Co. Ltd., AM 1.5, 100mW/cm²). Electron diffusion coefficient in TiO₂ layers was estimated with intensity modulated photocurrent spectroscopy (IMPS)¹⁵⁻¹⁷. These samples were exposed to 680 nm light by use of a laser diode (Lab Lasers, Coherent Japan Inc.). The laser diode was the source of both bias and

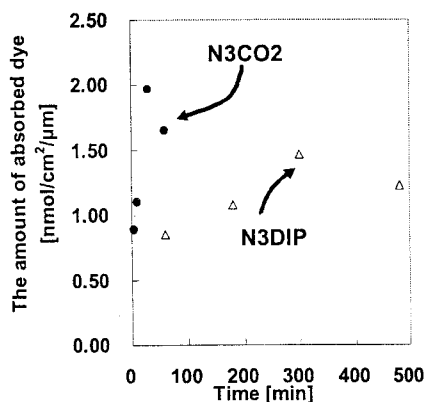


Figure 4. The amount of adsorbed dye vs. treated time

N3DIP: N3 dye was dipped at the pressure of the atmosphere

N3CO2: N3 dye was adsorbed under pressurized CO₂ modulated light. A NF Corporation frequency response analyzer Model 5020 was used to control light modulation and to measure the modulation of photo-potential. The current was measured by a Hokuto Denko Model HA-151 potentiometer. The amplitude of the sinusoidal modulation of

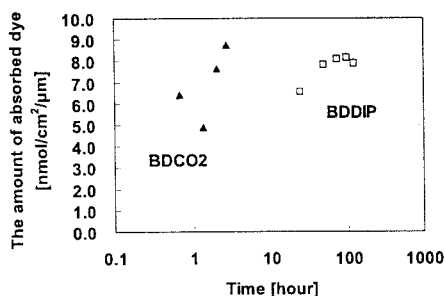


Figure 5. The amount of adsorbed dye vs. treated time

BDDIP: BD dye was dipped at the pressure of the atmosphere

BDCO2: BD dye was adsorbed under pressurized CO₂

the light intensity had an average value of 0.05 I₀. Electron diffusion coefficient (D_e) was estimated by the frequency of minimum imaginary component in IMPS complex plane plot (f_{min}) as follows: D_e=d²2πf_{min}, where, d stands for TiO₂ thickness. The amount of dyes adsorbed on TiO₂ layers were measured optically after the adsorbed dyes were dissolved in NaOH aqueous solution. The optical absorption at 504 nm was used for the calculation of the amount of dyes.

Figure 4 shows the relationship between the amount of N3 dyes adsorbed and adsorption time. The dye uptake in a pressurized CO₂ atmosphere was carried out much faster than that by a conventional dipping process. The time needed for N3 adsorption under a pressurized CO₂ atmosphere was shortened to 30 min. from 300 min. for dipping. In addition, dye concentration was higher than that prepared by the conventional dipping process. The time needed for black dye adsorption under a pressurized CO₂ atmosphere was

remarkably shortened to 70 min. from 6,000 min. for dipping (Figure 5). Nazeeruddin and his coworkers have reported swift N719 dye uptake by dipping heated TiO₂ substrates into dye solutions¹⁸. As far as we know, there is no report

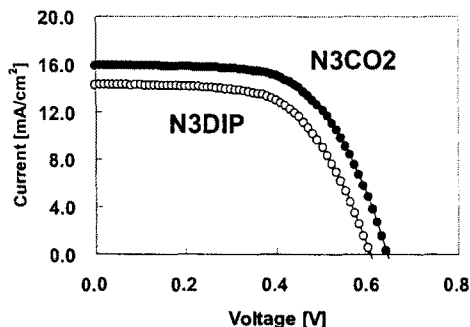


Figure 6. I-V curves for DSC prepared by dipping and under pressurized CO₂

on swift uptake of black dye. Figure 6 shows the I-V curves for DSCs prepared by a conventional dipping process and under a pressurized CO₂ atmosphere. Large increases in Jsc and Voc were observed for DCS prepared under a pressurized CO₂ atmosphere and one prepared by a conventional dipping process. Large increases in Jsc and Voc were observed again for DSC stained with black dye. Black dye is commonly adsorbed with co-adsorbents such as deoxycholic acid (DCA) in order to suppress black dye aggregation^{11,12}. DCA was not added in this experiment in order to avoid complicated factors because our objective is to clear the effect of a pressurized a CO₂ atmosphere.

Increases in Voc from 0.61 to 0.64 V for N3 dye and

Table 1 Photo-voltaic performances

	N3CO2	N3DIP	BDCO2	BDDIP
Efficiency(%)	6.31	5.39	8.76	7.10
ff	0.62	0.61	0.62	0.60
Voc (V)	0.64	0.61	0.69	0.63
Jsc (mA/cm ²)	15.93	14.29	20.66	18.96

N3CO2 and N3DIP: see Figure 4. BDCO2 and BDDIP: see Figure 5

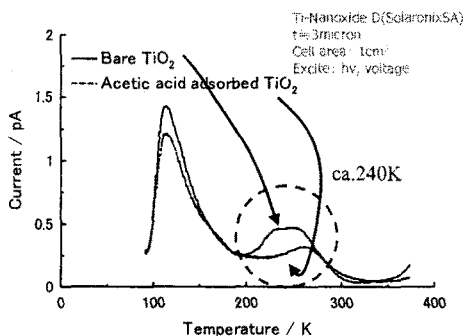


Figure 7. TSC spectrum with surface modification

from 0.63 to 0.69 V for black dye were explained by

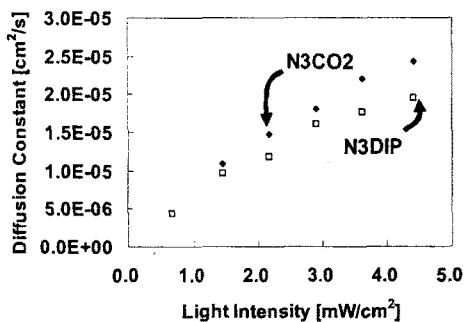


Figure 8. Diffusion coefficient vs. light intensity

retardation of back electron transfer reactions. This explanation was supported by decreases in dark currents. Better coverage of TiO₂ surface with dye molecules would retard back electron transfer reactions from TiO₂ layers to electrolytes. It has been reported that electron traps on the surface of TiO₂ nano-particles are one of the origin causing back electron transfer reactions from TiO₂ to I₂(I₃⁻) in electrolytes. In addition, these surface traps have been reported to disappear by adsorbing carboxylic acids on the TiO₂ layers¹⁹. We also observed disappearance of traps by observing thermally stimulated current (TSC). Figure 7 shows TSC curves of TiO₂ layers before and after acetic acid adsorption on TiO₂ layers. At 100 K, electron traps were buried with photo-generated electrons. As the temperature is raised at a certain rate, trapped electrons are released from the traps because of the thermal motions, which is recorded as current. Two peaks were observed at around 240 K before acetic acid adsorption (bare TiO₂). One of the peaks disappeared after the acetic acid was adsorbed on TiO₂ layers. Dye molecules have carboxylic acids and should act in the same way as carboxylic acid. This also supports the assumption that better coverage of TiO₂ nano-particles with dye molecules decreased the amount of surface traps and retarded back electron transfer reactions, resulting in the increase in Voc.

Increases in Jsc from 14.29 to 15.93 mA/cm² for N3 dye was also explained by the increase in the amount of dye molecules. Jsc also increased from 18.96 to 20.66 mA/cm² for black dye. It was found that electron diffusion coefficients increased when dyes were adsorbed in a

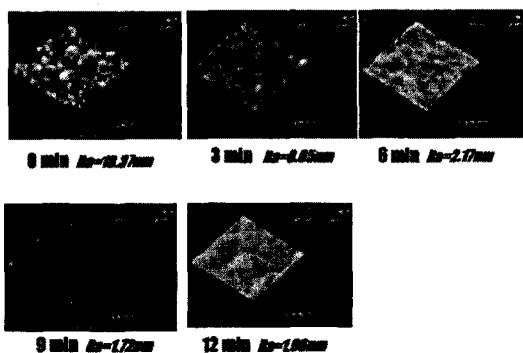


Figure 9. AFM image of low E glass after polishing

pressurized CO₂ atmosphere as shown in Figure 8. The increase in J_{sc} would be explained by the increase in dye concentration adsorbed on TiO₂ surfaces and the decreases in the amount of surface traps by the better coverage of TiO₂ surfaces with dye molecules^{19,20}.

CONTACT BETWEEN TRANSPARENT CONDUCIVE LAYER (TCL) AND TiO₂ LAYERS

Surfaces of transparent conductive layers have textures in order to scatter and confine sun light when they are used for Si based solar cells. The TCL may not be optimized for DSC application, because the light

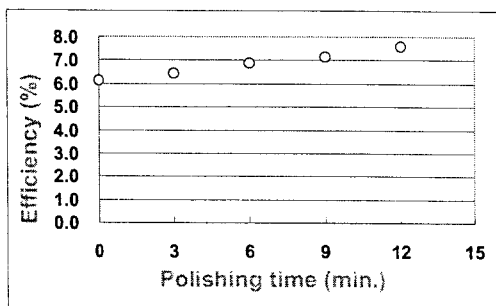


Figure 10. Polishing time vs. Efficiency

management is carried out by putting scattering layers in TiO₂ layers for DSCs.

We found that photo-conversion efficiency increased when surface of TCL glass was polished. Figure 9 shows the texture changes after a low E glass was polished. This had a texture of Ra:18.37 nm originally. When this was polished with a polisher containing nano-silica particles, the texture changed gradually and the surface was planed. Figure 10 summarizes the relationship between photo-conversion efficiency and the polishing time. The efficiency increased with an increase in the polishing time. Voc and ff did not change largely but J_{sc} increased with an increase in the polishing time, leading to the conclusion that J_{sc} increase was associated with the increase in photo-conversion efficiency. Considering the fact that interfacial resistances associated with TiO₂ electrodes, the effect caused by the polishing was concluded to be brought about by improved contact between TCL and TiO₂ nano-particles.

ION-PATH IN TiO₂ LAYERS

Sun-light conversion to electricity is carried out at the portion of TiO₂ layers which is close to TCL. Therefore, I⁻ has to diffuse into the bottom of TiO₂ layers to give electrons.

Table 1 Apparent diffusion coefficient in porous TiO₂ layers prepared by coating and ESC methods

Electrolyte	Apparent diffusion coefficient of I ₃ ⁻ (cm ² /s)	
	Coating	ESC
EL-AN	1.00 x 10 ⁻⁵	1.55 x 10 ⁻⁵
EL-IL	1.64 x 10 ⁻⁷	2.98 x 10 ⁻⁷

In addition, I₂(I₃⁻) has to diffuse out of the bottom to the surface of the TiO₂ layers. Because of this, continuous ion diffusion paths should be fabricated in the porous TiO₂ layers.

Coatings by a screen printing method are commonly employed for the film preparations²¹. Spray coatings are also employed for the film preparations²². However, ionic paths fabricated by these methods were thought to be random. We aimed at making the ionic path perpendicular to the substrate by use of electric fields. We now report that DSCs prepared by electro-spray methods show higher photocurrents than those prepared by conventional coating methods and the results may be associated with ionic path fabrication.

Electrolyte compositions and their abbreviations are as follows:

EL-AC: I₂ 40 mM, LiI 500 mM, t-butylpyridine 580 mM in acetonitrile;

EL-IL: I₂ 300 mM, LiI 500 mM, t-butylpyridine 580 mM in methylpropylimidazolium iodide containing 5 % of water.

Cells are abbreviated as follows:

EL-AC-ESC: Cells filled with EL-AC electrolyte and

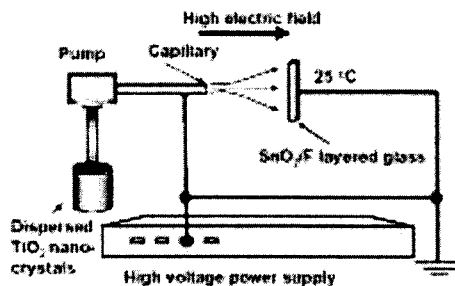


Figure 11. Electro-spray deposition of nano-TiO₂ particles fabricated by an electro-spray coating method;

EL-IL-COAT: Cells filled with EL-IL electrolyte and fabricated by a conventional method (Screen printing method). Figure 11 shows the apparatus employed. Figure 12 shows the relationship between photo-current and photo-

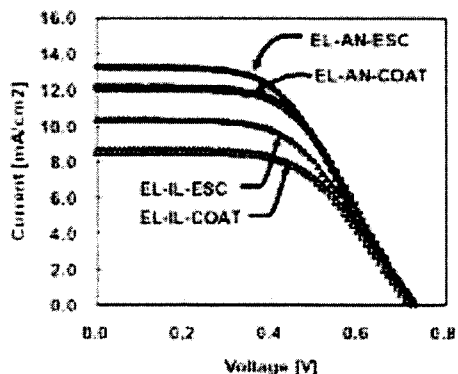


Figure 12. I-V curves for DSCs prepared by ESC and coating ESC: electro-spray coating, COAT: conventional coating voltage for DSCs prepared by an electro-spray method (ESC) and a screen printing method(COAT). Higher J_{sc} was observed when the TiO₂ layers were fabricated by a electro-

spray coating method for both electrolytes. The amount of dye molecules adsorbed, electron life time, electron diffusion coefficient and electron diffusion length on TiO₂ layers did not change largely between them.

Apparent limiting current and apparent diffusion coefficient of I₃⁻ within porous TiO₂ layers were measured relatively (Table 1). This clearly shows that the DSC prepared by the ESC technique has better ionic paths than that prepared by the conventional coating method. It is likely that the increase in J_{sc} is associated with the fabrication of better ion paths.

Chen and Schoonman have reported that fractal porous layers appeared when ceramic thin films were prepared with ESC methods in a certain condition as shown in Figure 13^{23,24}.

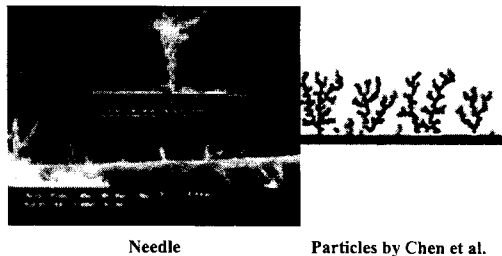


Figure 13. Electrostatic growth of TiO₂ needles and expected electrostatic growth of nano-particles

When TiO₂ needle shape crystals (TFL 100, Ishihara Techno Corp.) were electro-sprayed on F/SnO₂ conductive glasses, upward growing of TiO₂ needle bundles were observed besides standing of the TiO₂ needles on the conductive substrates. The upward growing shape of TiO₂ needle was similar to that reported by Chen and Schoonman (Figure 13 right). Considering the results reported by Chen and Schoonman, and our results using TiO₂ needles, some electrostatic interactions between flying TiO₂ nano-particles and TiO₂ nano-particles deposited on a conductive layer can be expected. It is reasonable to explain that electrostatic interactions between TiO₂ nano-particles during electro-spray depositions make the structures similar to that in Figure 13, where wide streams of ion paths (Main stream) and narrow streams of ion paths (Branches) are combined. The organized ion paths structure would retard the decrease in ion diffusions caused by TiO₂ nano-particles because the wide stream is expected to go through from the bottom of TiO₂ layer to the surface.

Conclusion

In order to increase photo-conversion efficiency for DSCs, we proposed the following items.

1) Better coverage of TiO₂ layers with dye molecules decreased surface electron traps, resulting in increasing J_{sc} and Voc. This was achieved by adsorption of dye molecules under a pressurized CO₂ atmosphere.

2) Contact between TCL and TiO₂ layers was improved by polishing TCL surfaces. J_{sc} increases were brought about by this better contact.

3) Fabrication of ionic paths in TiO₂ layers was one of the resolutions to improve the J_{sc} in some cases. The better ionic paths were fabricated by an electro-spray coating method.

References

1. B. O'Regan, M. Grätzel, *Nature*, 353, 737 (1991).
2. M. K. Nazeerudin, A. Kay, I. Rodicio, R. Humphry-Baker, E. Muller, P. Liska, N. Vlachopoulos, M. Grätzel, *J. Am. Chem. Soc.*, 115, 6382 (1993).
3. T. Renouard, R. -A. Fallahpour, M. K. Nazeeruddin, R. Humphry-Baker, S. I. Gorelsky, A. B. P. Lever, M. Grätzel, *Inorg. Chem.*, 41, 367 (2002).
4. R. Amadelli, R. Argazzi, C. A. Bignozzi, F. Scandola, *J. Am. Chem. Soc.*, 112, 7099 (1990).
5. Z. -S. Wang, C. -H. Huang, B. -W. Zhang, Y. -Y. Hou, P. -H. Xie, H. -J. Qian, K. Ibrahim, *New J. Chem.*, 24, 567 (2000).
6. Z. -S. Wang, F. -Y. Li, C. -H. Huang, L. Wang, M. Wei, L. -P. Jim, N. -Q. Li, *J. Phys. Chem., B*, 104, 9676 (2000).
7. Z. -S. Wang, K. Hara, Y. Dan-oh, C. Kasada, A. Shinpo, S. Suga, H. Arakawa, H. Sugihara, *J. Phys. Chem., B*, 109, 3907 (2005).
8. K. Hara, M. Kurashige, Y. Dan-oh, C. Kasada, A. Shinpo, S. Suga, K. Sayama, H. Arakawa, *New J. Chem.*, 27, 783 (2003).
9. Y. -G. Kim, J. Walker, L. A. Samuelson, J. Kumar, *Nano Lett.*, 3, 523 (2003).
10. G. K. R. Senadeera, K. Nakamura, T. Kitamura, Y. Wada, S. Yanagida, *Appl. Phys. Lett.*, 83, 5470 (2003).
11. M. K. Nazeeruddin, P. Pechy, T. Renouard, S. M. Zakeeruddin, R. Humphry-Baker, P. Comte, P. Liska, L. Cevey, E. Costa, V. Shklover, L. Spiccia, G. B. Deacon, C. A. Bignozzi, M. Grätzel, *J. Am. Chem. Soc.*, 123, 1613 (2001).
12. Z. -S. Wang, T. Yamaguchi, H. Sugihara, H. Arakawa, *Langmuir*, 21, 4272 (2005).
13. P. G. Jessop, T. Ikariya, R. Noyori, *Nature*, 368, 231 (1994).
14. K. K. Bando, Y. Mitsuzuka, M. Sugino, H. Sugihara, K. Sayama, H. Arakawa, *Chem. Lett.*, 853 (1999).
15. G. Schlichthorl, S. Y. Hung, J. Sprague, and A. J. Frank, *J. Phys. Chem. B*, 101, 8141 (1997).
16. L. M. Peter, and K. G. U. Wijayatha, *Electrochim. Acta.*, 45, 4543 (2000).
17. T. Yoshida, T. Oekermann, K. Okabe, D. Schlettwein, K. Funabiki, and H. Minoura, *Electrochem.*, 70, 470 (2002).
18. M. D. Nazeeruddin, R. Splivallo, P. Liska, P. Comte, and M. Grätzel, *Chem. Comm.*, 1456 (2003).
19. S. Nakade, Y. Saito, W. Kubo, T. Kanzaki, T. Kitamura, Y. Wada and S. Yanagida, *Electrochem. Commun.*, 5, 804 (2003).
20. S. Sakaguchi, H. Ueki, T. Kato, T. Kado, R. Shiratuchi, W. Takashima, K. Kaneto, and S. Hayase, *J. Photochem. Photobiol. A. Chem.*, 164, 117 (2004).
21. A. Hagfeldt and M. Grätzel, *Chem. Rev.*, 95, 49 (1995).
22. Satoshi Uchida, Miho Tomiha, Hirotozu Takizawa, and Masahide Kawaraya, *J. Photochem. & Photobiol. A: Chemistry*, 164, 93 (2004).
23. C. C. Chen and J. Schoonman, *NATO Sci. Ser. E.*, 295 (2000).
24. C. C. Chen, E. M. Kelder, P. J. J. M. van der Put, and J. Schoonman, *J. Mater. Chem.*, 6, 765 (1996).